

# *In vivo* one-photon confocal calcium imaging of neuronal activity from the mouse neocortex

Satoshi Iwasaki<sup>a</sup> and Yuji Ikegaya<sup>a,b,\*</sup>

<sup>a</sup> Graduate School of Pharmaceutical Sciences, The University of Tokyo, Tokyo 113-0033, Japan

<sup>b</sup> Center for Information and Neural Networks, National Institute of Information and Communications Technology, Suita City, Osaka, 565-0871, Japan

Received 15 January 2018

Accepted 25 July 2018

**Abstract.** *In vivo* calcium imaging is a powerful tool used to record neuronal activity from living animals. For this purpose, two-photon excitation laser-scanning microscopy is commonly used because of the optical accessibility of deep tissues. In this study, we report that one-photon confocal scanning laser microscopy, when optimally tuned, is also applicable for *in vivo* calcium imaging from the superficial layer of the neocortex. By combining a Nipkow-disk confocal unit with a fluorescence stereo zoom microscope and a high numerical aperture objective, we succeeded in recording the fluorescence signal of individual cells at a depth of up to 160  $\mu\text{m}$  in brain tissues, which corresponds to layer II of the mouse neocortex. In fact, we conducted *in vivo* functional multineuron calcium imaging and simultaneously recorded spontaneous activity from more than 100 neocortical layer II neurons. This one-photon confocal system provides a simple, low-cost experimental platform for time-lapse imaging from living animals.

Keywords: *In vivo*, calcium, Nipkow-disk confocal microscopy, spinning-disk confocal microscopy, living animal

## 1. Introduction

Functional calcium imaging is one of the powerful tools that are widely used to record neuronal spiking activity in multiple neurons with high temporal and spatial resolution. This technique is useful even when it is applied to living animals, which have intact anatomical structures in the neuronal network and are expected to produce more natural activity than *in vitro* preparations. For *in vivo* neuronal imaging, two-photon excitation laser-scanning fluorescence microscopy provides good optical penetration into deep brain tissues and becomes more advantageous when used in light-scattering mammalian brains [3,8,11]. Despite its high optical accessibility, two-photon microscopy may be inconvenient because of, for example, its complex optical system, narrow fields of view, and difficulty in conducting simultaneous electrophysiological recordings. To overcome these problems, one might use one-photon microscopy for *in vivo* calcium imaging [5]; however, conventional one-photon epi-fluorescence imaging requires high

---

\*Corresponding author: Yuji Ikegaya, PhD, Laboratory of Chemical Pharmacology, Graduate School of Pharmaceutical Sciences, The University of Tokyo, 7-3-1 Hongo, Bunkyo-ku, Tokyo 113-0033, Japan. Tel.: +81-3-5841-4780; Fax: +81-3-5841-4786; E-mail: [yuji@ikegaya.jp](mailto:yuji@ikegaya.jp).

light powers for fluorophore excitation and often results in rapid photobleaching and severe phototoxicity. Moreover, data obtained by conventional epi-fluorescence imaging are inevitably contaminated by out-of-focus signals, reducing the signal-to-noise ratios.

In the present study, we developed an *in vivo* one-photon confocal laser-scanning imaging method that captures neocortical neurons in living mice with single-cell resolution. Our previous work demonstrated that Nipkow-disk confocal microscopy is capable of obtaining fluorescence signal at a depth of up to 150  $\mu\text{m}$  from brain tissues *in vitro* [13]. We now combined this Nipkow-disk confocal scanner unit with a microscope that has a high numerical aperture (NA) objective and an efficient photon detector and examined its optical accessibility using *in vivo* functional multineuron calcium imaging (fMCI).

## 2. Methods

### 2.1. Animal ethics

Experiments were performed with the approval of the animal experiment ethics committee at the University of Tokyo (approval number: P29-11) and according to the University of Tokyo guidelines for the care and use of laboratory animals. These experimental protocols were carried out in accordance with the Fundamental Guidelines for Proper Conduct of Animal Experiment and Related Activities in Academic Research Institutions (Ministry of Education, Culture, Sports, Science and Technology, Notice No. 71 of 2006), the Standards for Breeding and Housing of and Pain Alleviation for Experimental Animals (Ministry of the Environment, Notice No. 88 of 2006) and the Guidelines on the Method of Animal Disposal (Prime Minister's Office, Notice No. 40 of 1995). All animals were housed under a 12-h dark–light cycle (light from 07:00 to 19:00) at  $22 \pm 1^\circ\text{C}$  with *ad libitum* food and water.

### 2.2. Imaging apparatus

Images were obtained using an upright zoom microscope (Axio Zoom.V16; Carl Zeiss, Oberkochen, Germany) equipped with an objective lens (Plan-NEOFLUAR Z 2.3 $\times$ , NA: 0.57, Working distance: 56 mm; Carl Zeiss), a Nipkow-disk confocal scanner unit (CSU-W1; Yokogawa Electric, Tokyo, Japan), and a water-cooled, electron-multiplying charge-coupled device (EMCCD) camera (iXon Ultra DU897U; Andor Technology, Belfast, UK), which were regulated by Andor iQ software (Andor). Fluorophores were excited at 488 nm and 561 nm using a laser combiner (LBC2-UTI-2; PNEUM, Saitama, Japan) and were visualized with 525-nm and 617-nm bandpass emission filters, respectively. The laser power was set to 5–10 mW.

### 2.3. Assessment of the depth of optical accessibility

Adult thy1-mGFP transgenic C57B6 mice (gifted from Dr. V. de Paola and Dr. P. Caroni), which express membrane-targeted green fluorescent protein (mGFP), were used [1]. A craniotomy over the neocortex was performed as previously described [2]. Briefly, mice were anesthetized with urethane (1.0–1.5 g/kg, *i.p.*). The skull was exposed and glued to a metal head-holding plate. A craniotomy with a 1- to 2-mm diameter (AP =  $-3.8$  mm, LM = 2.0 mm from bregma) was performed over the primary visual cortex (V1), and the dura was surgically removed. The exposed cortical surface was treated for 15 min with 100  $\mu\text{M}$  sulforhodamine 101 (SR101, Invitrogen, Carlsbad, USA), a fluorescent marker for astrocytes [7]. SR101 was dissolved in artificial cerebrospinal fluid (aCSF) that consisted of the

following (in mM): 127 NaCl, 26 NaHCO<sub>3</sub>, 1.6 KCl, 1.24 KH<sub>2</sub>PO<sub>4</sub>, 1.3 MgSO<sub>4</sub>, 2.4 CaCl<sub>2</sub>, and 10 glucose. After washing with aCSF, mGFP and SR101 were excited at 488 nm and 561 nm, respectively. Images at both wavelengths were taken at a 20- $\mu$ m Z-step from the surface. To quantify the optical accessibility, we calculated the Fano factors for the fluorescent intensities of all pixels in a given confocal image. The Fano factor is defined as

$$\text{Fano factor} = \frac{\sigma^2}{\mu}$$

where  $\sigma^2$  is the variance and  $\mu$  is the mean value. The Fano factor becomes higher when the signal-to-noise ratio is high.

#### 2.4. Recording ongoing activity with fMCI

Postnatal 21- to 28-day-old wild-type ICR mice (Japan SLC, Shizuoka, Japan) were anesthetized with urethane (1.0–1.5 g/kg, i.p.), and the V1 surface was exposed as described above. Cortical neurons were loaded with Oregon Green 488 BAPTA-1AM (OGB-1; Invitrogen) under visual guidance with the zoom microscope. OGB-1 was dissolved at 10 mM in DMSO with 10% PowerLoad™ (Invitrogen) and was diluted to a concentration of 1 mM with aCSF containing 100  $\mu$ M SR101. OGB-1 was injected with an air pressure of 100–500 mbar for 30 s into the V1 at a depth of 100–150  $\mu$ m from the surface through a glass pipette [2]. The pipette was then carefully removed, and a glass cover slip (Matsunami Glass, Tokyo, Japan) was placed on the craniotomized area. After incubating the samples for 40–60 min, the OGB-1 fluorescence was imaged from the V1 layer II neurons. OGB-1 and SR101 were laser-excited at wavelengths of 488 nm and 561 nm, respectively. Images (1,024  $\times$  1,024 pixels, 16 bit) were captured at 10 Hz. The fluorescence intensity of OGB-1 was measured using ImageJ software (NIH) and was normalized by the mean intensity of the entire OGB-1-diffused area. For each cell, the change in fluorescence intensity ( $\Delta F/F$ ) was measured as  $(F_t - F_0)/F_0$ , where  $F_t$  is the fluorescence intensity at time  $t$ , and  $F_0$  is the baseline fluorescence intensity from  $-10$  s to  $10$  s relative to  $t$ . To calculate  $F_0$ , fluorescence intensities lower than the median value was extracted, and the remaining data were averaged.  $\Delta F/F$  was then denoised using the Okada-filter [9]. Calcium transients were semiautomatically detected using machine learning and were inspected by well-trained human analysts [10,12].

#### 2.5. Data analysis of multineuronal activity

Shannon index (SI) quantifies the dispersion of components in a histogram [15]. SI was calculated as previously described [14]. Briefly, SI is defined as

$$\text{SI} = - \sum_i \left( \frac{k_i}{K} \right) \log_2 \left( \frac{k_i}{K} \right)$$

where  $K$  is the total number of components, and  $k_i$  is the number of components in the  $i$ th bin (bin: 1 s). SI was then normalized with the maximal ( $\text{SI}_{\max}$ ) and minimal values ( $\text{SI}_{\min}$ ), which were obtained through data shuffle with maintaining  $K$  and bin.  $\text{SI}_{\max}$  is given when components are as evenly redistributed as possible, whereas  $\text{SI}_{\min}$  is given when components are as biased as possible. Then normalized

SI (NSI) is defined as

$$\text{NSI} = \frac{\text{SI} - \text{SI}_{\min}}{\text{SI}_{\max} - \text{SI}_{\min}}$$

NSI takes a value from 0 to 1. Higher NSI means more dispersive. Then, we obtained  $\text{logit}(\text{NSI})$  as followed:

$$\text{logit}(\text{NSI}) = \log\left(\frac{\text{NSI}}{1 - \text{NSI}}\right)$$

For each dataset, we compared  $\text{logit}(\text{NSI})$  of real data with those of their surrogates, in which the same number of calcium events were reallocated across neurons and video frames. We generated 10,000 surrogates for every 30-s window and estimated their 95% confidence intervals.

### 3. Results

#### 3.1. Assessment of the depth of optical accessibility

We combined the Nipkow-disk confocal unit CSU-W1 with an Axio Zoom.V16 zoom microscope and an iXon Ultra DU897U cooled EMCCD camera (Fig. 1A). First, we assessed the optically accessible depth of this optical system using thy1-mGFP mice, which express mGFP in a few neocortical neurons, mainly in layer V. The mice were anesthetized with urethane, and their heads were fixed to a custom-made stereotaxic fixture (Fig. 1B). The skull and the dura over the V1 surface were removed, and SR101 was applied to the cortical surface. The fluorescence of mGFP and SR101 was detectable at depths of up to 160  $\mu\text{m}$  from the pia surface, although their signal-to-noise ratios decreased as a function of depth

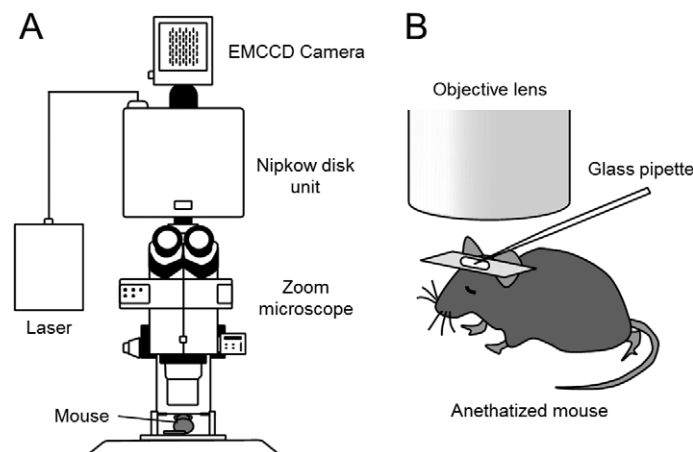


Fig. 1. Schematic illustration of *in vivo* Nipkow-disk confocal imaging. (A) Diagram of the set up used in this work. A Nipkow-disk confocal scanner unit (Yokogawa CSU-W1) and an EMCCD camera (Andor iXon Ultra DU897U) are equipped on a zoom microscope (Carl Zeiss Axio Zoom.V16). (B) Enlarged view around a specimen. A mouse was anesthetized with urethane and was head-fixed to a stereotaxic frame. Neocortical neurons were loaded with dyes through a glass pipette. The fluorescence was corrected through an objective lens (Carl Zeiss Plan-NEOFLUAR Z 2.3 $\times$ ).

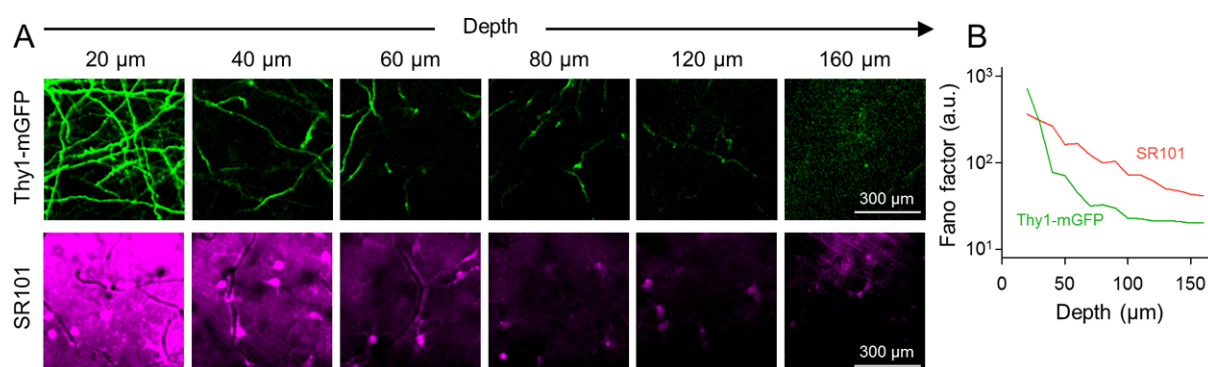


Fig. 2. Assessment of the depth of optical accessibility. (A) Representative images of mGFP and SR101 at various depths from the V1 pia surface. SR101 was applied on the cortical surface of thy1-mGFP mice. (B) Fano factor of fluorescent intensity of each pixel. Fano factor became lower in deeper tissue.

(Fig. 2). Because principal neurons in the most superficial part of the neocortical layer II are usually located within this accessible depth, we expected that our one-photon optical system could capture the fluorescence signal from layer II cortical neurons.

### 3.2. Recording neuronal activity with fMCI

We then applied this technique to *in vivo* fMCI. Wild-type mice were anesthetized, and the V1 area was craniotomized. The fluorescent calcium indicator OGB-1 and SR101 were injected through a glass pipette into layer II. The microscope Axio Zoom.V16 carrying the 2.3× objective lens Plan-NEOFLUAR Z utilizes continuously different magnifications ranging from 16× to 258×, which cover microscopic fields ranging from 900 × 900 μm<sup>2</sup> to 14 × 14 mm<sup>2</sup>. In fact, it was able to simultaneously image approximately 3,000 SR101-labeled astrocytes in a single microscopic field at depths of more than 100 μm (Fig. 3A left). Because we used the high-resolution camera iXon Ultra DU897U with an EMCCD array of 1,024 × 1,024 pixels, we were able to separate individual astrocytes at the single-cell level (Fig. 3A right). For OGB-1 fluorescence, we were able to image 150–200 layer II cells within a diameter of approximately 400 μm where OGB-1 was bolus-loaded (Fig. 3B left). As OGB-1 fluorescence also had single cell resolution (Fig. 3B right), we conducted time-lapse calcium imaging from the cell population at a rate of 10 frames per second. We observed spontaneous calcium transients in the somata of these cells (Fig. 4A–C). To examine whether these transients reflected neuronal activity, we analyzed their synchronicity using information theory (SI) [14]. Resampling comparisons revealed that the real logit(NSI) values were consistently lower than the chance levels in all 10 datasets. Thus, calcium transients were significantly synchronized among neurons and thus were expected to reflect physiological neuronal activity (Fig. 4D).

## 4. Discussion

Although two-photon excitation fluorescence microscopy is the first choice for *in vivo* calcium imaging because of its efficient light penetration, the Nipkow-disk confocal microscopy is also capable of

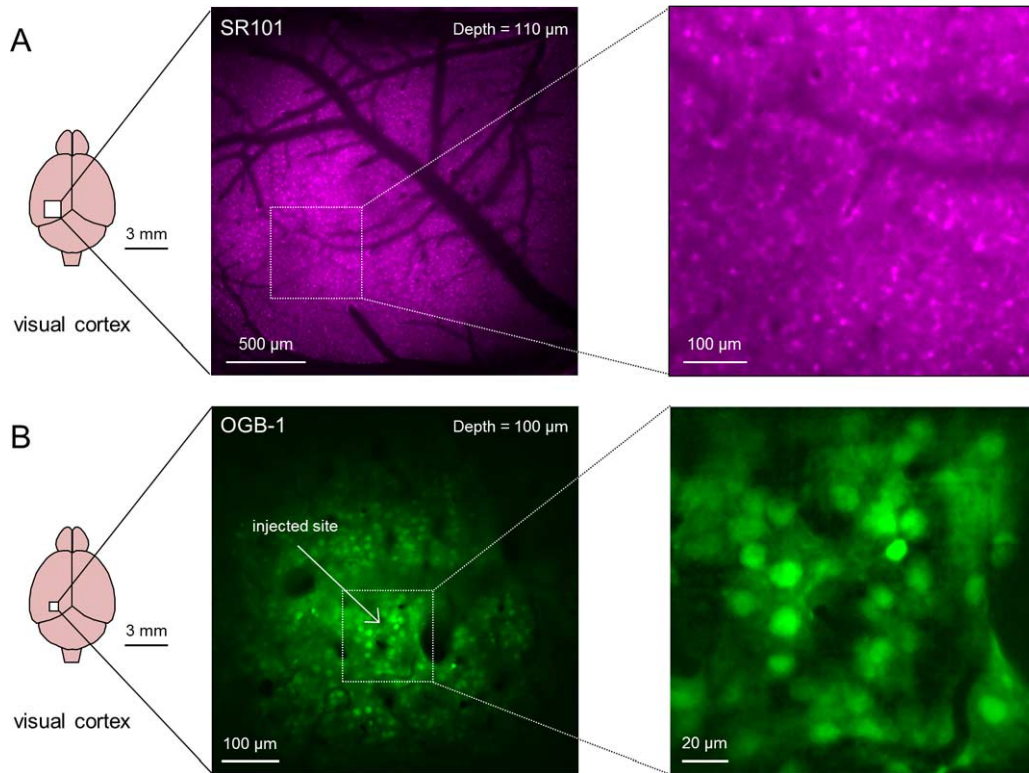


Fig. 3. *In vivo* confocal imaging. (A) Astrocytes labeled with SR101 were imaged at a depth of  $110\ \mu\text{m}$  from a  $3.2 \times 3.2\ \text{mm}^2$  of the V1 region in layer II, a part of which is magnified in the right inset. (B) Cells labeled with OGB-1 were imaged at a depth of  $100\ \mu\text{m}$  from a  $900 \times 900\ \mu\text{m}^2$  of the V1 layer II, and the boxed region is magnified in the right inset. Note that the cells were visualized with single-cell resolution.

assessing at a depth of up to  $150\ \mu\text{m}$ , presumably because of its efficient light detection [13]. In the present study, which combined a Nipkow-disk unit with a zoom microscope, we showed that one-photon confocal laser-scanning microscopy is also able to assess tissues deep enough to observe calcium activity from individual neocortical neurons in living mice.

#### 4.1. Comparison to two-photon microscopy

Two-photon microscopy is advantageous in visualizing cells in deep brain regions, including the hippocampus and the medial prefrontal cortex [4,6]. However, its apparatus is relatively complex and expensive, and its long-term maintenance may be laborious even for experts. Moreover, the working distance of its objective is often too short to simultaneously record electrophysiological signal using glass electrodes, such as local field potential and intracellular potentials. Compared to the conventional two-photon microscopy, our one-photon confocal system is easier to operate and is less expensive. The zoom microscope has long working distances of more than  $5\ \text{cm}$ , and its wide field of vision covers more than  $10 \times 10\ \text{mm}^2$ . Therefore, it enables simultaneously recording calcium activity and electrical activity from several brain regions. One of its disadvantages is the optical depth limit of less than  $200\ \mu\text{m}$ , which cannot access neocortical L5 neurons, the hippocampus or the medial prefrontal cortex.

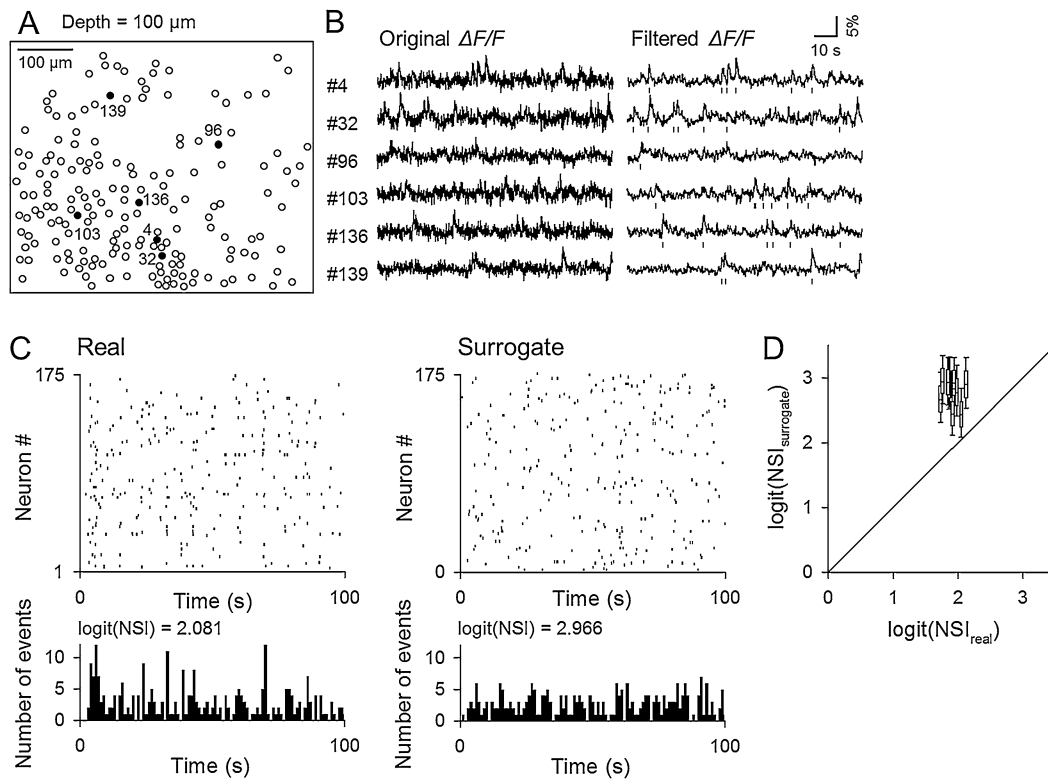


Fig. 4. *In vivo* fMRI. (A) A spatial map of the cells identified in Fig. 3B. (B) Representative raw traces of the fluorescence intensity in neurons numbered in the panel A (left) were denoised (right). Blue dots below the traces indicate the event times of putative spiking activity of the neurons (right). (C) (left, top) A representative raster plot for calcium activity of all 175 neurons shown in the panel A. Each dot indicates the onset time of a single calcium event exhibited by the corresponding neuron. (bottom) logit(NSI) in multineuronal  $\text{Ca}^{2+}$  events. A histogram at time was made, so that logit(NSI) evaluate the event synchrony. (right) An example of surrogate data, in which same number of  $\text{Ca}^{2+}$  events were allocated to randomly selected neurons and time. (D) Comparison between logit(NSI)<sub>real</sub> and logit(NSI)<sub>surrogate</sub>. Ten 30-s windows were placed at a randomly selected time and ten thousand surrogates were obtained from each data. logit(NSI)<sub>real</sub> was always lower than logit(NSI)<sub>surrogate</sub>.

#### 4.2. Comparison to epi-fluorescence microscopy

A recent elegant report demonstrated that more than 1,000 neurons could simultaneously be imaged *in vivo* using one-photon epi-fluorescence microscopy, in which the excitation light power was raised up to 50 mW to visualize neurons in the deep tissues of the mouse neocortex [5]. In our confocal imaging, less than 10 mW of laser excitation was sufficient to image neocortical layer II cells. Therefore, our system is expected to produce less phototoxic and longer recordings. In preliminary experiments, we obtained images again 30 min after the first recording session and found that the cell bodies and their calcium transients were still detectable at a comparable level to the first recording session. More importantly, confocal imaging excludes out-of-focus fluorescent lights through pinholes, achieving high signal-to-noise ratios.

#### 4.3. Conclusion

In this work, which combined a Nipkow-disk unit and a zoom microscope, we showed that one-photon confocal microscopy is capable of imaging neuronal activity from living animals. Our system is easier to

handle and more economical than multi-photon microscopy and exhibits lower phototoxicity and higher signal-to-noise ratios than a one-photon epi-fluorescence microscope. These results indicate that our one-photon confocal microscope has potential usefulness in *in vivo* functional neuronal imaging.

### Conflict of interest

None to report.

### Acknowledgements

This work was supported by Grants-in-Aid for Scientific Research (26250003; 25119004) and the Human Frontier Science Program (RGP0019/2016). This work was partly conducted as a program in the International Research Center for Neurointelligence (WPI-IRCN) at the University of Tokyo Institutes for Advanced Study at the University of Tokyo.

### References

- [1] V. De Paola, S. Arber and P. Caroni, AMPA receptors regulate dynamic equilibrium of presynaptic terminals in mature hippocampal networks, *Nat Neurosci* **6** (2003), 491–500. doi:[10.1038/nn1046](https://doi.org/10.1038/nn1046).
- [2] K. Funayama, G. Minamisawa, N. Matsumoto, H. Ban, A.W. Chan, N. Matsuki et al., Neocortical rebound depolarization enhances visual perception, *PLoS Biol* **13** (2015), e1002231. doi:[10.1371/journal.pbio.1002231](https://doi.org/10.1371/journal.pbio.1002231).
- [3] R. Kawakami, K. Sawada, Y. Kusama, Y.C. Fang, S. Kanazawa, Y. Kozawa et al., In vivo two-photon imaging of mouse hippocampal neurons in dentate gyrus using a light source based on a high-peak power gain-switched laser diode, *Biomed Opt Express* **6** (2015), 891–901. doi:[10.1364/BOE.6.000891](https://doi.org/10.1364/BOE.6.000891).
- [4] R. Kawakami, K. Sawada, A. Sato, T. Hibi, Y. Kozawa, S. Sato et al., Visualizing hippocampal neurons with in vivo two-photon microscopy using a 1030 nm picosecond pulse laser, *Sci Rep* **3** (2013), 1014. doi:[10.1038/srep01014](https://doi.org/10.1038/srep01014).
- [5] T.H. Kim, Y. Zhang, J. Lecoq, J.C. Jung, J. Li, H. Zeng et al., Long-term optical access to an estimated one million neurons in the live mouse cortex, *Cell Rep* **17** (2016), 3385–3394. doi:[10.1016/j.celrep.2016.12.004](https://doi.org/10.1016/j.celrep.2016.12.004).
- [6] M. Kondo, K. Kobayashi, M. Ohkura, J. Nakai and M. Matsuzaki, Two-photon calcium imaging of the medial prefrontal cortex and hippocampus without cortical invasion, *Elife* **6** (2017), e26839.
- [7] A. Nimmerjahn, F. Kirchhoff, J.N. Kerr and F. Helmchen, Sulforhodamine 101 as a specific marker of astroglia in the neocortex in vivo, *Nat Methods* **1** (2004), 31–37. doi:[10.1038/nmeth706](https://doi.org/10.1038/nmeth706).
- [8] K. Ohki, S. Chung, Y.H. Ch'ng, P. Kara and R.C. Reid, Functional imaging with cellular resolution reveals precise micro-architecture in visual cortex, *Nature* **433** (2005), 597–603. doi:[10.1038/nature03274](https://doi.org/10.1038/nature03274).
- [9] M. Okada, T. Ishikawa and Y. Ikegaya, A computationally efficient filter for reducing shot noise in low S/N data, *PLoS One* **11** (2016), e0157595. doi:[10.1371/journal.pone.0157595](https://doi.org/10.1371/journal.pone.0157595).
- [10] T. Sasaki, N. Takahashi, N. Matsuki and Y. Ikegaya, Fast and accurate detection of action potentials from somatic calcium fluctuations, *J Neurophysiol* **100** (2008), 1668–1676. doi:[10.1152/jn.00084.2008](https://doi.org/10.1152/jn.00084.2008).
- [11] C. Stosiek, O. Garaschuk, K. Holthoff and A. Konnerth, In vivo two-photon calcium imaging of neuronal networks, *Proc Natl Acad Sci USA* **100** (2003), 7319–7324. doi:[10.1073/pnas.1232232100](https://doi.org/10.1073/pnas.1232232100).
- [12] A.F. Szymanska, C. Kobayashi, H. Norimoto, T. Ishikawa, Y. Ikegaya and Z. Nenadic, Accurate detection of low signal-to-noise ratio neuronal calcium transient waves using a matched filter, *J Neurosci Methods* **259** (2016), 1–12. doi:[10.1016/j.jneumeth.2015.10.014](https://doi.org/10.1016/j.jneumeth.2015.10.014).
- [13] Y. Takahara, N. Matsuki and Y. Ikegaya, Nipkow confocal imaging from deep brain tissues, *J Integr Neurosci* **10** (2011), 121–129. doi:[10.1142/S0219635211002658](https://doi.org/10.1142/S0219635211002658).
- [14] A. Usami, N. Matsuki and Y. Ikegaya, Spontaneous plasticity of multineuronal activity patterns in activated hippocampal networks, *Neural Plast* **2008** (2008), 108969. doi:[10.1155/2008/108969](https://doi.org/10.1155/2008/108969).
- [15] R.I.B.W. Wilson, *A Primer of Population Biology*, Sinauer Associates, Stamford, CT, USA, 1971.